"PEGylated DX-1000: Pharmacokinetics and antineoplastic activity of a specific plasmin inhibitor"

Devy, Laetitia ; Rabbani, Shafaat A. ; Stochl, Mark ; Ruskowski, Mary ; Mackie, Ian ; Naa, Laurent ; Toews, Mark ; van Gool, Reinoud ; Chen, Jie ; Leyz, Art ; Ladner, Robert C. ; Dransfield, Daniel T. ; Henderikx, Paula

Abstract

Novel inhibitors of the urokinase-mediated plasminogen (plg) activation system are potentially of great clinical benefit as anticancer treatments. Using phage display, we identified DX-1000 a tissue factor pathway inhibitor-derived Kunitz domain protein which is a specific high-affinity inhibitor of plasmin (pln) (K-i = 99 pM). When tested in vitro, DX-1000 blocks plasmin-mediated pro-matrix metalloproteinase-9 (proMMP-9) activation on cells and dose-dependently inhibits tube formation, while not significantly affecting hemostasis and coagulation. However, this low-molecular weight protein inhibitor (similar to 7kDa) exhibits rapid plasma clearance in mice and rabbits, limiting its potential clinical use in chronic diseases. After site-specific PEGylation, DX-1000 retains its activity and exhibits a decreased plasma clearance. This PEGylated derivative is effective in vitro, as well as potent in inhibiting tumor growth of green fluorescent protein (GFP)-labeled MDA-MB-231 cells. 4PEG...

Document type : *Article de périodique (Journal article)*

Neoplasia • Vol. 9, No. 11, November 2007, pp. 927–937 927

www.neoplasia.com

PEGylated DX-1000: Pharmacokinetics and Antineoplastic Activity of a Specific Plasmin Inhibitor

Laetitia Devy, Shafaat A. Rabbani†, Mark Stochl‡, Mary Ruskowski§, Ian Mackie¶, Laurent Naa*, Mark Toews‡, Reinoud van Gool*, Jie Chen‡, Art Ley‡, Robert C. Ladner‡, Daniel T. Dransfield‡ and Paula Henderikx**

*Dyax S.A. Building 22, Boulevard du Rectorat 27B, Sart-Tilman, B-4000 Liege 1, Belgium; †Department of Medicine, McGill University Health Centre, Montreal, QC, Canada; ‡Dyax Corp., 300 Technology Square, Cambridge, MA, USA; §Division of Nuclear Medicine, Department of Radiology, University of Massachusetts Medical School, Worcester, MA 01655-0243, USA; ¶Haematology Department, University College London, London, UK

Abstract

Novel inhibitors of the urokinase-mediated plasminogen (plg) activation system are potentially of great clinical benefit as anticancer treatments. Using phage display, we identified DX-1000 a tissue factor pathway inhibitor–derived Kunitz domain protein which is a specific high-affinity inhibitor of plasmin (pln) (K_i = 99 pM). When tested *in vitro*, DX-1000 blocks plasmin-mediated pro-matrix metalloproteinase-9 (proMMP-9) activation on cells and dose-dependently inhibits tube formation, while not significantly affecting hemostasis and coagulation. However, this low–molecular weight protein inhibitor (~7 kDa) exhibits rapid plasma clearance in mice and rabbits, limiting its potential clinical use in chronic diseases. After site-specific PEGylation, DX-1000 retains its activity and exhibits a decreased plasma clearance. This PEGylated derivative is effective *in vitro*, as well as potent in inhibiting tumor growth of green fluorescent protein (GFP)–labeled MDA-MB-231 cells. 4PEG–DX-1000 treatment causes a significant reduction of urokinase-type plasminogen activator (uPA) and plasminogen expressions, a reduction of tumor proliferation, and vascularization. 4PEG–DX-1000 treatment significantly decreases the level of active mitogen-activated protein kinase (MAPK) in the primary tumors and reduces metastasis incidence. Together, our results demonstrate the potential value of plasmin inhibitors as therapeutic agents for blocking breast cancer growth and metastasis.

Neoplasia (2007) **9,** 927–937

Keywords: Plasmin inhibitor, matrix metalloproteinases, PEGylation, plasma clearance, antineoplastic agent.

Introduction

Plasmin (pln), a 90-kDa broad-spectrum protease of tryptic specificity, plays a central role in the fibrinolytic process in regulating the turnover of extracellular matrix (ECM) components [1–3]. Pln is present in the blood in its inactive zymogen form plasminogen (plg) [4]; its active form being rapidly inhibited in the systemic circulation by α_2-antiplasmin and α_2-macroglobulin [5]. Conversion of plg to active pln is catalyzed by urokinase-type plasminogen activator (uPA) or tissue-type plasminogen activator (tPA). Whereas tPA is accepted to be primarily involved in thrombolysis, it is mainly uPA that generates active pln leading to local ECM breakdown [6–8]. The uPA bound to the membranous urokinase-type plasminogen activator receptor (uPAR) increases plg activation and subsequent pln-dependent proteolysis [9–11]. When pln is bound to the cell surface, it is protected from α_2-antiplasmin–mediated inhibition confining proteolysis locally at or near the cell surface [11–13]. Pln plays a major role in pathologic conditions such as inflammation, tumor cell growth, and metastasis formation [7,14]. Invasive properties of tumor cells may be at least partially dependent on direct pln-mediated proteolysis of the ECM [15] and indirectly dependent on the activation of latent pro-matrix metalloproteinases (proMMPs) and collagenases by pln [9,16–18]. The pln cascade may activate MMP-3 and MMP-9 through the uPA/uPAR complex at the cell surface accelerating the tumorigenic effects [17,19]. Pln induces the permeability of blood vessels [20] and thereby facilitates the systemic dissemination of tumor cells.

Pln and MMPs may also play additional roles in angiogenesis [21–23] by releasing specific matrix-derived growth factors including basic fibroblast growth factor and vascular endothelial growth factor [24] and in the activation of latent transforming growth factor–beta [25–27], insulin-like growth factor-1, and insulin-like growth factor–binding protein. Moreover, endothelial cells at the leading edge of a new blood vessel

Abbreviations: ANOVA, analysis of variance; ECM, extracellular matrix; FCS, fetal calf serum; HPLC, high-performance liquid chromatography; HUVEC, Human umbilical vein endothelial cell; MAPK, mitogen-activated protein kinase; MMP-2, matrix metalloproteinase 2; MMP-3, matrix metalloproteinase 3; MMP-9, matrix metalloproteinase 9; MMP, matrix metalloproteinase; PEG, poly(ethylene glycol); plg, plasminogen; pln, plasmin; pMAPK, phosphorylated MAPK; SE-HPLC, size-exclusion high-performance liquid chromatography; TFPI, tissue factor pathway inhibitor; tPA, tissue-type plasminogen activator; uPA, urokinase-type plasminogen activator; uPAR, urokinase type plasminogen activator receptor

Address all correspondence to: Laetitia Devy, PhD, Dyax S.A. Building 22, Boulevard du Rectorat 27B, Sart-Tilman, B-4000 Liege 1, Belgium. E-mail: ldevy@dyax.com

Received 3 July 2007; Revised 4 September 2007; Accepted 7 September 2007.

DOI 10.1593/neo.07544

express components of both pln and MMP systems and their expression is regulated by the same growth factors and cytokines [28]. Thus, pln is an attractive target for cancer therapy because: (a) this enzyme is predominantly present in its inactive zymogen form, with its active form being mostly present locally in tissues undergoing remodeling, e.g. tumors; (b) it is one of the major enzymes directly and/or indirectly involved in degradation of the ECM; and (c) it stimulates angiogenesis.

We have described the use of phage display to identify a human Kunitz domain–based inhibitor of human pln [29]. The protein, DX-1000, is a potent (K_i = 99 pM) and highly specific inhibitor of pln. Because of its low molecular weight, the protein exhibits a rapid plasma clearance rate *in vivo*. Therefore, we prolonged *in vivo* circulation time of DX-1000 by conjugation with poly(ethylene glycol) (PEG). In the present work, we demonstrate the specificity of DX-1000 for pln, its minor effect on hemostasis and coagulation *in vitro*, and its potency *in vitro* as an antiproteolytic and antiangiogenic agent. We also describe the PEGylated derivative of DX-1000 (4PEG–DX-1000), its *in vitro* and *in vivo* inhibitory properties, its slow clearance, and its high stability.

Materials and Methods

Production and Purification of DX-1000

DX-1000 (7167 Da) was produced and purified as described previously [29].

Hemostasis Studies

Blood from healthy donors was collected in trisodium citrate (Vacutainer; Becton Dickinson, Oxford, UK) and plasma was prepared by centrifugation at 2000*g* for 15 minutes. *Fibrinolysis* was measured by Euglobulin Clot Lysis Time and fibrin plate lysis (Dr Ian Mackie, Hematology Department, University College London, London, UK), using standard techniques in the presence and absence of 5 μg/ml dextran sulfate. Fibrin plates were prepared using plg-rich fibrinogen (Quadratech Ltd, Epsom, UK) and bovine thrombin (Diagnostic Reagents Ltd, Oxford, UK), in six-well culture plates standardized using Reference Plasma 100% (Technoclone Ltd, Dorking, UK). *Plasma clot lysis* was studied using 0.5 μM rec-tPA (Quadratech) and citrated plasma with thrombin and $CaCl_2$ (0.7 U/ml and 0.6 mM, respectively) in a microplate [30]. The formation and dissolution of the clot were monitored as the serial change in optical density at 405 nm. The time taken to reach 50% lysis was calculated graphically. *Prothrombin time* (Innovin; Dade Behring, Marburg, Germany, or PT-Fib HS Plus; Instrumentation Laboratory, Lexington, MA), *thrombin time* (Thromboclotin; Dade Behring), *activated partial thromboplastin time* (APTT) (Actin FS, Actin FSL, or Pathromtin SL; Dade Behring), and *Clauss fibrinogen* (Thrombin Reagent; Dade Behring) were measured using an analyzer (CA-7000; Sysmex, Kobe, Japan). *Whole blood clotting time* was measured using unanticoagulated, fresh whole blood on a coagulometer (KC4A Amelung; Trinity Biotech, Bray, Ireland). *Platelet function* was studied using a platelet function analyzer (PFA-100; Dade Behring). *Thrombelastography* (*TEG*) was studied using citrated blood at 30 to 120 minutes from venepuncture, in the presence of kaolin, using a thrombelastographic analyzer (TEG-5000; Medicell, London, UK) and then recalcification. In some experiments, 1 μg/ml tPA (Quadratech) was added to induce fibrinolysis at the time of mixing with kaolin.

Plasminogen assays were performed using streptokinase and the amidolytic substrate *H*-D-Val-Leu-Lys-OH.pNA (Channel Diagnostics, Walmer, UK) in a microtiter technique. Protein C was assayed using an activator (Protac) and the amidolytic substrate Unitrate PC, 2AcOH.H-D-Lys(Cbo)-Pro-Arg-pNA (Technoclone Ltd). The effect of DX-1000 on activated protein C (rAPC, a kind gift of Eli-Lilly, Indianapolis, IN) activity was studied in a microtiter amidolytic assay using 6.2 μg/ml (rAPC) and Unitrate PC substrate.

Preparation of PEGylated DX-1000

DX-1000 in PBS was reacted with a 40-fold molar excess of methoxy-PEG-succinimidyl propionate (mPEG-SPA, M_r 5000; Shearwater Polymers, Huntsville, AL), in terms of total primary amino groups of DX-1000, at 4°C for 3 hours. The reaction was stopped with a 10-fold molar excess of glacial acetic acid. The 4PEG–DX-1000 was characterized by SDS-PAGE, analytical size-exclusion high-performance liquid chromatography (SE-HPLC), and mass analysis using matrix-assisted laser desorption/ionization time of flight. The specific inhibitory activity of DX-1000 after PEGylation was determined as previously described [29]. Briefly, DX-1000 and 4PEG–DX-1000 were incubated with 2 nM human pln at 30°C for 1 hour. Then, *N*-succinyl-Ala-Phe-Lys 7-amido-4-methylcoumarin acetate (Sigma-Aldrich, St. Louis, MO) was added to a final concentration of 100 μM. Measurements were taken on a Gemini plate reader with excitation at 360 nm and emission read at 460 nm. Plots of enzymatic rate *versus* inhibitor concentration were generated by nonlinear regression using SigmaPlot 8.0 to obtain K_i estimates:

$$\%\text{Activity} = 100 - \left(\frac{K_i\text{DX1000} + E) - \sqrt{(K_i\text{DX1000} + E)^2 - 4 \cdot \text{DX1000} \cdot E}}{2 \cdot E} \right) \cdot 100$$

where:

K_i = inhibition constant
DX1000 = total DX-1000 concentration
E = total human pln concentration (determined by active site titration)

Endotoxin levels of purified 4PEG–DX-1000 were measured using a commercially available Limulus Amebocyte Lysate (LAL) kinetic turbidimetric/PyroTurb ES (Glucoshield) method (Associates of Cape Cod, Inc., E. Falmouth, MA) and were consistently < 0.2 endotoxin units/mg.

Cell-Based Assays and Gel Zymography

Cells and cell culture HT-1080, MDA-MB-231, and HL-60 cells were obtained from the American Type Culture Collection (Rockville, MD). HT-1080 cells were cultured in

complete medium [RPMI 1640, 25 mM Hepes (Cambrex, Verviers, Belgium), 10% heat-inactivated fetal calf serum (FCS) (Life Technologies – Invitrogen SA, Merelbeke, Belgium), 2% amphotericin B (Fungizone; Life Technology – Invitrogen), and 1% penicillin–streptomycin (Life Technologies – Invitrogen)]. HL-60 cells were grown in RPMI supplemented with 25 mM Hepes and 15% heat-inactivated FCS. Cultures were maintained at a cell concentration between 1×10^5 and 1×10^6 per ml. Cells transfected with green fluorescent protein (MDA-MB-231–GFP) were cultured as previously described [31]. Human umbilical vein endothelial cells (HUVECs) were freshly isolated from umbilical cords and cultured on gelatin-coated culture dishes in RPMI 1640 with 25 mM Hepes supplemented with growth factors (EGM SingleQuots; Cambrex), 200 mM L-glutamine, 1% penicillin–streptomycin, and 10% FCS. LEII mouse lung endothelial cells were a generous gift from Dr. Kari Alitalo, University of Helsinki. They were cultured in minimum essential medium containing Glutamax and Earl's Salts (Gibco, Life Technologies – Invitrogen) supplemented with 10% FCS.

Gelatin zymography. Gelatinolytic activities were analyzed by zymography as previously described [32]. Briefly, HL-60 cells (2×10^5) were grown for 24 hours, washed twice in PBS and incubated in the presence or absence of pln (10 mU/ml) and proMMP-3 (10 nM) in serum-free medium (Ultraculture medium; Cambrex) supplemented with 1% L-glutamine and 1% penicillin–streptomycin. In some conditions, DX-1000 or 4PEG–DX-1000 (1 μM) was added to block pln activity. After 48 hours, conditioned media were collected and concentrated 10-fold using centrifugal filter units (Centricon YM-30 columns; Millipore, Brussels, Belium). Then samples (30 μg protein/sample) were diluted in nonreduced SDS sample buffer and proteins were resolved by electrophoresis in 10% SDS–polyacrylamide gels copolymerized with 1 mg/ml gelatin. Gels were washed with 2.5% Triton X-100 for 1 hour and twice in Tris–HCl (pH 8.0) for 15 minutes at room temperature. The gels were incubated with substrate buffer [50 mM Tris–HCl (pH 8.0) and 10 mM $CaCl_2$] for 18 hours at 37°C. The gels were then stained with Coomassie brilliant blue R-250 and destained until clear bands of lysis appeared. Conditioned medium from HT-1080 cells treated with 20 ng/ml phorbol 12-myristate acetate served as a standard. To confirm the lytic bands, gels were treated with 20 mM EDTA (a metalloproteinase inhibitor) in the substrate buffer for 18 hours at 37°C.

Casein zymography. Serum-free samples were prepared as above and loaded onto gels containing β-casein as substrate (Zymo Blue Casein Gel; Invitrogen). On staining with Coomassie brilliant blue and destaining, the final gel had a uniform background except in regions to which serine proteases had migrated and cleaved the casein. Recombinant uPA served as a positive control. Molecular standards were used to calibrate molecular weights.

Tube formation assay. HUVECs (passage 2) were seeded at 6×10^4/100 μl per well on collagen gel (50 μl of rat tail collagen type I, 1.5 mg/ml; Serva, Belgium) in culture medium and allowed to spread for 1.5 hour. The cells then were covered with a new layer of collagen type I (1.5 mg/ml, new preparation, 50 μl/well). After polymerization of the gel, culture medium was added to each well in the presence or absence of increasing concentrations of DX-1000 or 4PEG–DX-1000 (ranging from 0.1 nM to 10 μM). Mouse LEII lung endothelial cells were seeded at a density of 2×10^4 cells/well on top of a Matrigel layer according to the manufacturer's guidelines (BD Biosciences, Bedford, MA). Culture medium was added to each well in the presence or absence of appropriate concentrations of DX-1000 or 4PEG–DX-1000. Cells were incubated at 37°C and 5% CO_2 for 16 to 18 hours.

Tube length quantification and IC_{50} determination. Endothelial cell tube formation was assessed with an inverted photomicroscope. Microphotographs of the center of each well at low power were taken with a camera (Nikon; Nikon Belux, Brussels, Belgium). Tube formation in the microphotographs was quantitatively analyzed (total tube length) with an imaging software (MetaVue, Downingtown, PA). Tube formation of untreated HUVECs was used as a negative control. The assay was performed three times in triplicate. SigmaPlot 8.0 was used to determine IC_{50} values.

Animal Protocols

All animal protocols were in accordance with and approved by the institutional review board. For *in vivo* pharmacokinetics and stability studies of DX-1000 and 4PEG–DX-1000, normal female BALB/c mice and naive New Zealand White rabbits were used. The radiolabeled preparations (IODO-GEN; Pierce Chemical Company, Rockford, IL) [33,34] were injected into the mice through the tail vein and into the rabbits through an ear vein. At predetermined times postadministration, animals were sacrificed and blood samples were taken for radiation counting to determine clearance rates and for SE-HPLC on Superose 12 (Amersham Biosciences, Pittsburgh, PA) to test for stability. Specific accumulation of ^{125}I–DX-1000 and ^{125}I–4PEG–DX-1000 in mouse liver, heart, kidney, lung, spleen, stomach, intestine, and muscles were also assessed. Data on *in vivo* pharmacokinetic parameters obtained from rodents and rabbits were extrapolated to humans by interspecies scaling [35,36].

For xenograft studies, 4- to 6-week-old female BALB/c mice (National Cancer Institute, Fredrick, MD) were used. Before inoculation, cultured MDA-MB-231–GFP were washed with Hank's balanced buffer and centrifuged at 1500 rpm for 5 minutes. Cell pellets (5×10^5 cells/mouse) were resuspended in 100 μl of Matrigel (Becton Dickinson Labware) and saline mixture (20% Matrigel) and injected subcutaneously into the mammary fat pad of mice. All animals were numbered and kept separately in a temperature-controlled room on a 12-hour/12-hour light/dark schedule with food and water *ad libitum* [31,37]. Tumors were allowed to grow and randomized to average volume of 60 to 70 mm^3 in each group and treated with 4PEG–DX-1000 (0.1, 1, and 10 mg/kg every day) or vehicle alone through intraperitoneal route for 4 weeks from the time of randomization of animals.

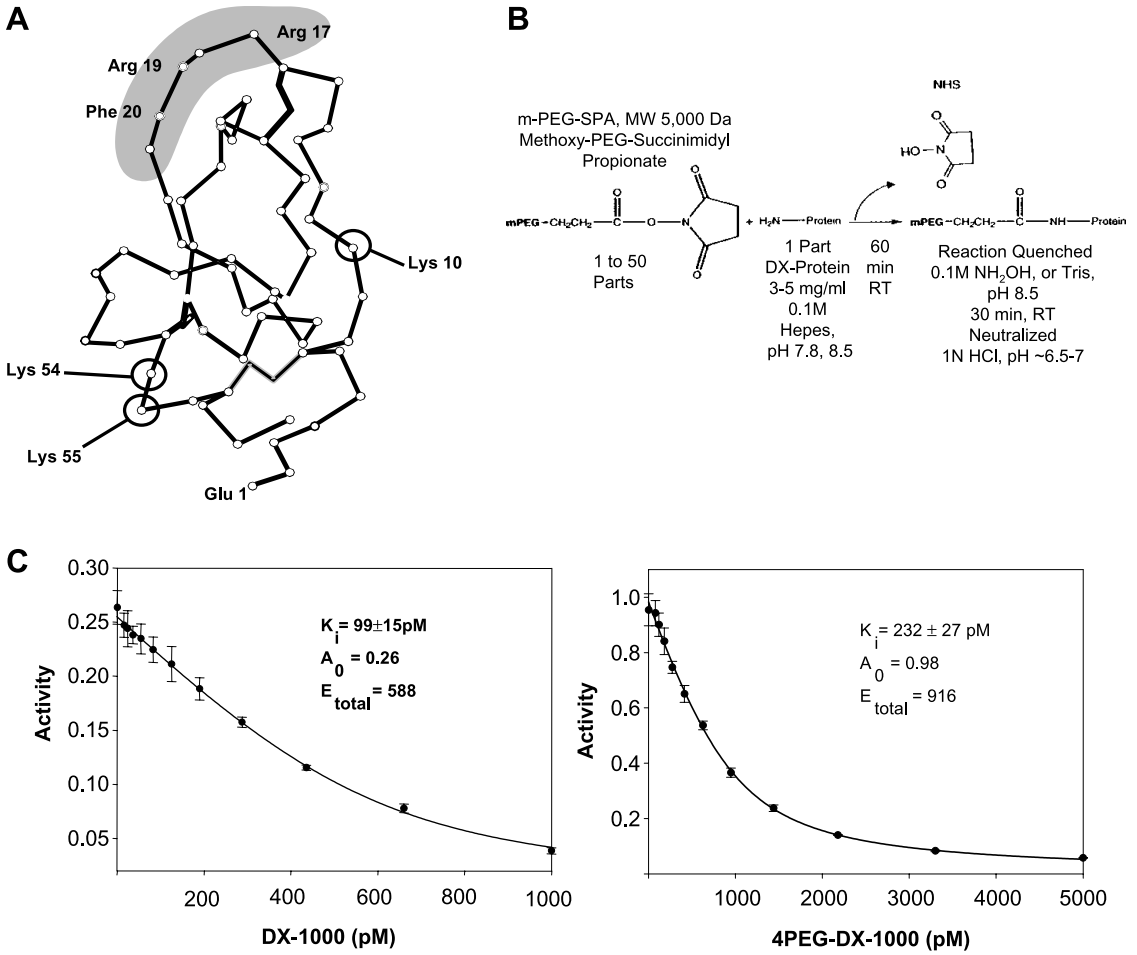

Figure 1. *PEGylation scheme and activity measurements. (A) Model of the structure of DX-1000. The locations of Lys-10, Lys-54, and Lys-55 are shown. (B) PEGylation scheme. (C) K_i measurements for the inhibition of human pln by DX-1000 (left-hand panel) and 4PEG–DX-1000 (right-hand panel). Closed circles show measured values for activity. For each sample, the solid line shows the fit of the equation for a tight binding inhibitor by nonlinear regression. The values for total active enzyme (E_{total}) and K_i obtained from each fit are shown.*

All animals were monitored for any potential side effects throughout the course of these studies. Tumor volumes were determined from caliper measurement at weekly intervals by two independent observers blinded to experimental groups.

Administration was discontinued after 4 weeks, the animals were sacrificed and their lungs, liver, and spleen as well as the primary tumors were removed for further analysis. Lungs, liver, and spleen were sliced to 1-mm-thick slices of fresh tissue for direct examination under the fluorescent microscope for the presence of GFP-expressing tumor foci. The number of GFP-expressing tumor foci per field of examination was counted as previously described [37].

Immunohistochemistry

Immunohistochemistry was carried out as previously described using the avidin–biotin–peroxidase complex method [38,39]. The antibodies used were monoclonal antibodies against CD31 (1:50) (Santa Cruz Biotechnology Inc., Santa Cruz, CA); Ki-67 (1:100) (Dako, Carpinteria, CA); uPA (1:50) (American Diagnostica Inc., Stamford, CT); plg (American Diagnostica Inc.); and rabbit polyclonal antibodies against mitogen-activated protein kinase (MAPK) and phosphorylated MAPK (pMAPK; 1:50) (Cell Signaling Technology, Beverly, MA) overnight at 4°C [37–39]. Biotinylated goat anti–mouse or goat anti–rabbit antibodies (Vector Laboratories Inc., Burlingame, CA) were used as the secondary antibodies at 1:200 for 30 minutes at room temperature. The slides were treated with Vectastain ABC-AP kit (Vector Laboratories Inc.) (1:200) for 30 minutes at room temperature. The signals were visualized with Fast Red TR/Naphthol AS-MX phosphate (Sigma-Aldrich) containing 1 mM levamisole for 10 to 15 minutes. The sections were then counterstained with hematoxylin (Fisher Scientific, Ltd., Nepean, ON, Canada) and mounted with Kaiser's glycerol jelly. All sections were washed three times, 10 minutes each, with Tris buffer (pH 7.6) after each step. Negative controls included substitution of the primary antibody with PBS. Immunostaining of all tissues was quantitatively analyzed by using a computer-assisted image analysis system as previously described [40].

Statistical Analysis

Results are expressed as means ± SEM of at least triplicate determinations and statistical comparisons are based on Student's *t* test and analysis of variance (ANOVA). A P value of $< .05$ was considered significant.

Results

DX-1000 Has Potent Plasmin Inhibitory Activity

DX-1000 inhibits pln with high affinity (K_i = 99 pM) [29,41] and shows no significant inhibition of human uPA (K_i ~ 60 μM) or tPA (K_i ~10 μM). DX-1000 does not crossreact with human plasminogen. DX-1000 also inhibits pln from mouse, rat, rabbit, and chicken (K_i ~ 100 pM).

DX-1000 Does Not Significantly Affect Hemostasis and Coagulation In Vitro

When DX-1000 was added to plasma before euglobulin precipitation, no significant inhibition of clot lysis was observed using doses of up to 700 nM. In thrombelastography experiments, there was a small, but nonsignificant increase in the lag (*r*) time, but clotting time, rate, and maximal amplitude remained within the normal range, using 140 to 560 nM DX-1000. In the presence of tPA, fibrinolysis was inhibited in a dose-dependent manner [Ly30 for control, 140, 280, and 560 nM DX-1000 (mean ± SD): 71 ± 21, 64 ± 24, 46 ± 35 (P < .05), and 23 ± 16 (P < .001); Ly60: 86 ± 9, 82 ± 12, 67 ± 24 (P < .05), and 46 ± 22 (P < .005)]. We did not observe an effect of DX-1000 on prothrombin time, thrombin time, or Clauss fibrinogen assays at doses up to 5.6 μM. There were no significant effects of DX-1000 on activated partial thromboplastin time at concentrations up to 700 nM. No clinically significant effects of DX-1000 were observed on platelet function or whole blood coagulation time and we observed no interference in plasma assays of plg or protein C, as well as an absence of inhibition of activated protein C.

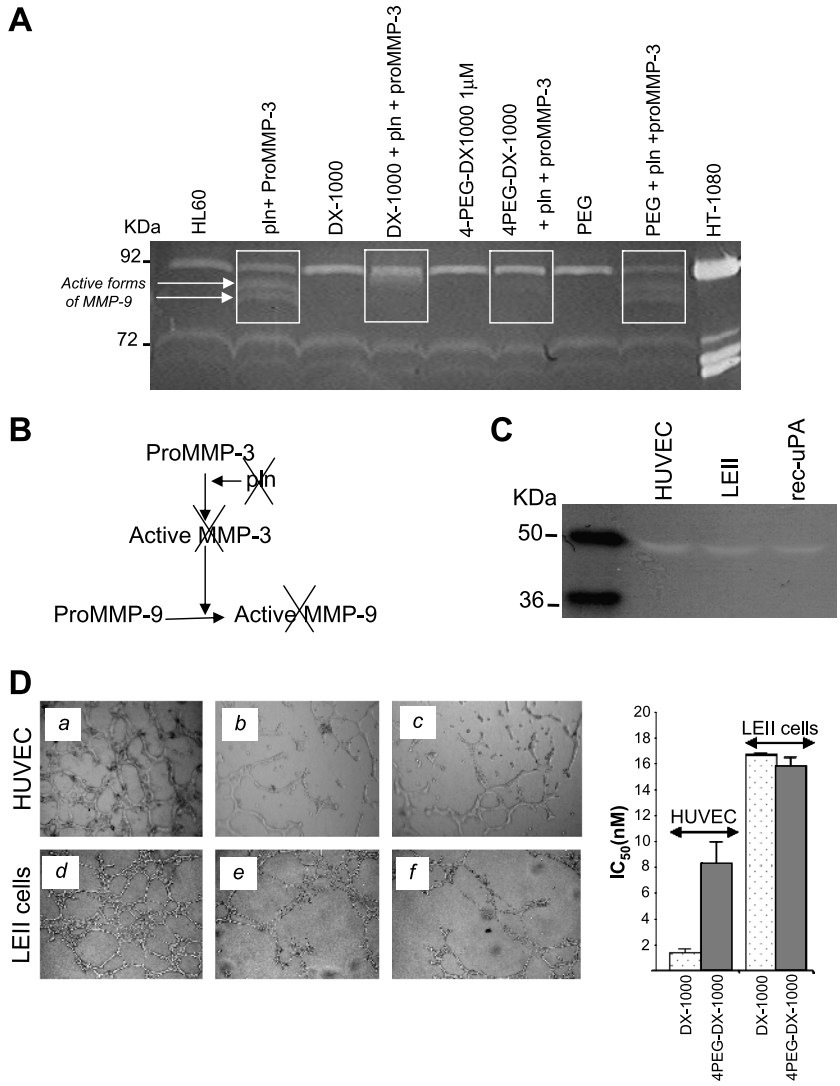

Figure 2. *Evaluation of DX-1000 and 4PEG–DX-1000 in cell-based assays. (A) Modulation of proMMP-9 activation. Gelatin zymogram of media conditioned by HL-60 cells cultured in the presence or absence of 4PEG–DX-1000 (1 μM) DX-1000 (1 μM) with or without plasmin (10 mU/ml) and proMMP-3 (10 nM). Conditioned medium of HT-1080 cells treated with phorbol 12-myristate acetate (20 ng/ml) was used to identify the gelatinolytic species. (B) Scheme depicting the blocking effect of DX-1000 or 4PEG–DX-1000 (illustrated by crosses) on proMMP-9 activation in HL-60 cells. (C) Expression of uPA by endothelial cells. Casein zymogram of media conditioned by LEII cells or HUVEC. Recombinant uPA (rec-uPA) was used as a positive control. Molecular standards were used to calibrate molecular weights. (D) Inhibitory effect of DX-1000 and 4PEG–DX-1000 on tube formation of HUVECs and LEII cells. Representative photomicrographs (left-hand panel) show three-dimensional cultures of HUVEC treated with (a) vehicle alone, (b) DX-1000 (10 nM), or (c) 4PEG–DX-1000 (10 nM) and three-dimensional cultures of mouse LEII cells treated with (d) vehicle alone, (e) DX-1000 (10 nM), or (f) 4PEG–DX-1000 (10 nM). IC_{50} values for DX-1000 and 4PEG–DX-1000 inhibition of tube formation (right-hand panel). Results are the means ± SEM of three such experiments.*

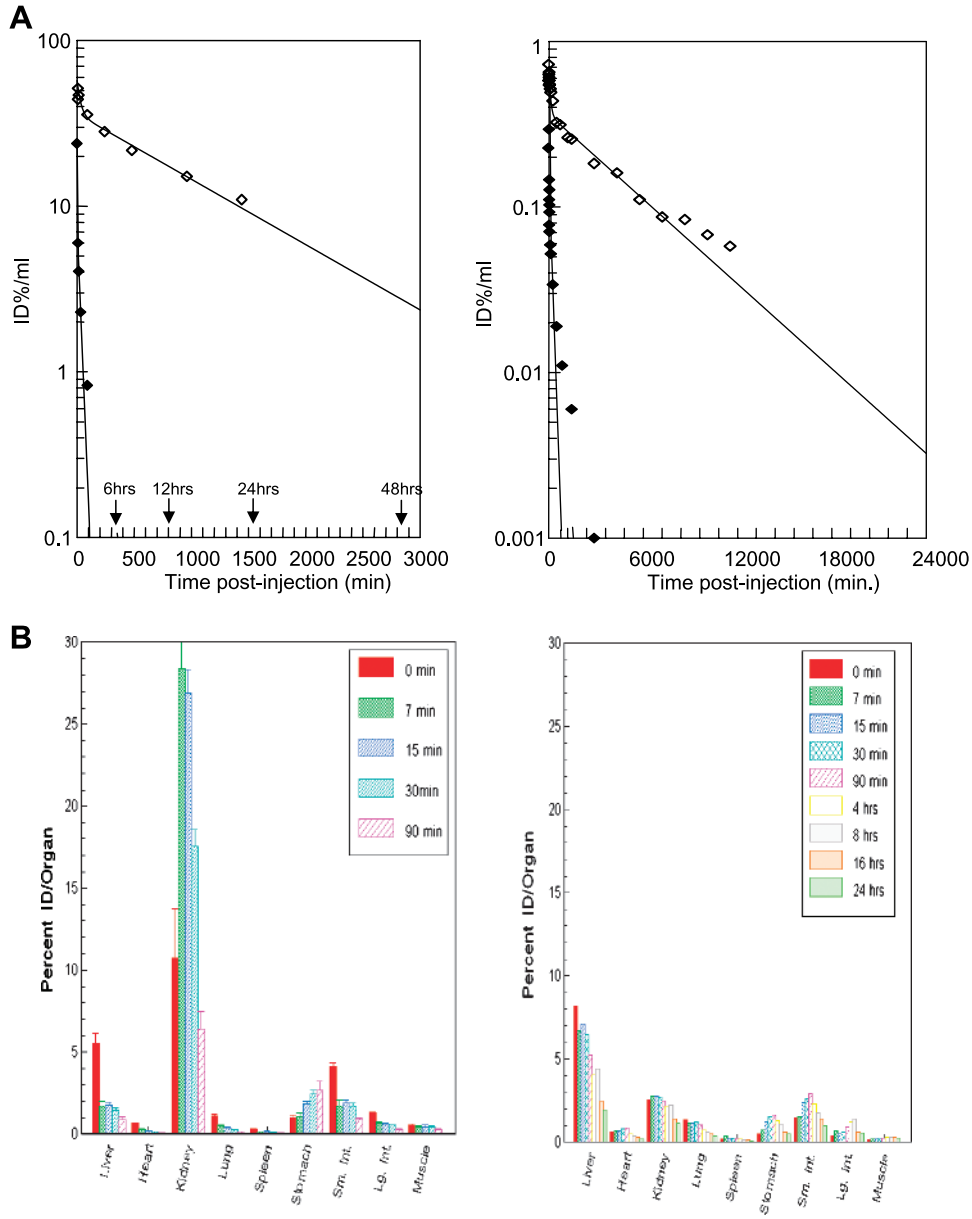

Figure 3. *Pharmacokinetics of DX-1000 and 4PEG–DX-1000 after intravenous injection in mice and rabbits. (A)* In vivo *plasma clearance curves for* ^{125}*I-labeled DX-1000 (closed diamonds) and for 4PEG–DX-1000 (diamonds) in mice (left-hand panel) and rabbits (right-hand panel). For in vivo pharmacokinetics studies, normal female BALB/c mice and naive New Zealand White rabbits were used. The radiolabeled preparations were injected into the mice through the tail vein and into the rabbits through an ear vein. At predetermined times postadministration, animals were sacrificed and blood samples were taken for radiation counting to determine clearance rates. Data are calculated as percent-injected dose per milliliter plasma (%ID/ml) and are presented as a function of elapsed time postadministration in minutes. The %ID/ml data are plotted on a logarithmic scale. The solid curve through each set of data is the four-parameter, least-squares fits to the data of the biexponential equation:* $y = Ae^{-\alpha t} + Be^{-\beta t}$. *(B) Biodistribution of* ^{125}*I–DX-1000 (left-hand panel) and* ^{125}*I–4PEG–DX-1000 (right-hand panel) in mice. Insert within each panel shows time point. Sm. Int., small intestine; Lg. Int., large intestine.*

Aprotinin was used as a reference reagent; it demonstrated inhibition of pln and activated protein C, inhibited clot lysis, and prolonged the activated partial thromboplastin time, in line with its known effects.

4PEG–DX-1000 Remains a Potent Inhibitor of Plasmin

We used amine reactive chemistry to couple 5-kDa PEG moieties specifically to four sites on DX-1000: three lysine residues (at positions 10, 54, and 55) and the amino-terminus. All four PEGylation sites are positioned distal to the portion of the inhibitor that interacts with pln (Figure 1, *A* and *B*). The final PEGylated DX-1000 (4PEG–DX-1000) molecule was purified by gel filtration HPLC. SDS-PAGE analysis demonstrated purity levels of approximately 100%. Matrix-assisted laser desorption/ionization time of flight analysis confirmed the expected mass of the 4 × 5 kDa PEGylated DX-1000 product to be ~27,600 Da. Whereas PEGylation increased the K_i value for plasmin by 2.5-fold (K_i = 99 pM for DX-1000; K_i = 232 pM for 4PEG–DX-1000) (Figure 1*C*), it remained a potent inhibitor of plasmin.

Table 1. Mouse Plasma Clearance.

Compound	α Phase Clearance (%)	α Phase Half-Life (minutes)	β Phase Clearance (%)	β Phase Half-Life	
				Minutes	Hours
DX-1000	87	1.5	13	26.9	0.45
4PEG–DX-1000	38	18	62	750	12.5

DX-1000 and 4PEG–DX-1000 Block Plasmin-Mediated proMMP-9 Activation in Tumor Cells

MMPs are produced as zymogen and it has been suggested that physiological activation of proMMP-9 involves pln. HL-60 cells constitutively produced significant amounts of proMMP-9 (Figure 2*A*, *lane 1*). Treatment of HL-60 cells with pln (10 mU/ml) and proMMP-3 (10 nM) led to the processing of endogenous proMMP-9 to active MMP-9 (Figure 2*A*, *lane 2*). ProMMP-9 remained latent after treatment of the cells with DX-1000 or 4PEG–DX-1000 alone (Figure 2*A*, *lanes 3 and 5*) or a combination of DX-1000 (or 4PEG–DX-1000) with pln and proMMP-3 (Figure 2*A*, *lanes 4 and 6*). PEG alone did not show any effect (Figure 2*A*, *lanes 7 and 8*). These results show the potency of DX-1000 and 4PEG–DX-1000 to efficiently inhibit plasmin-mediated activation of proMMP-9 in HL-60 cells (illustrated in Figure 2*B*).

DX-1000 and 4PEG–DX-1000 Inhibit Tube Formation By Endothelial Cells

During angiogenesis, endothelial cells use uPA to migrate and degrade the basement membrane surrounding capillary blood vessels. Casein zymography revealed constitutive expression of uPA in both human and mouse endothelial cells (HUVEC and LEII cells) (Figure 2*C*). Endothelial cells have the ability to form capillary-like structures when they are embedded in a 3D matrix, i.e., collagen for HUVEC (Figure 2*D*, *a*) and Matrigel for mouse LEII cells (Figure 2*D*, *d*). Treatment with DX-1000 or 4PEG–DX-1000 inhibited tube formation of HUVEC (Figure 2*D*, *b* and *c*) (IC_{50} = 1.4 ± 0.3 nM for DX-1000 and 8.3 ± 1.6 nM for 4PEG–DX-1000) and of LEII cells (Figure 2*D*, *e* and *f*) (IC_{50} = 16.6 ± 0.1 nM for DX-1000 and 15.8 ± 0.6 nM for 4PEG–DX-1000).

PEGylation of DX-1000 Substantially Decreases Plasma Clearance in Rodents

The pharmacokinetic properties of DX-1000 were typical for a Kunitz domain protein with a rapid clearance from the circulation (β phase half-life = 27 minutes in mice and 1 hour in rabbits) (Figure 3*A*; Tables 1 and 2). PEGylation of DX-1000 substantially decreased the clearance rate in mice with the β phase half-life increasing by about 25-fold in mice (Figure 3*A*, *left-hand panel*; Table 1) and nearly 60-fold in rabbits (Figure 3*A*, *right-hand panel*; Table 2). Biodistribution studies in mice showed that 4PEG–DX-1000 did not accumulate into the kidneys, in contrast to DX-1000 (Figure 3*B*). SE-HPLC analyses of plasma samples taken from mice and rabbits demonstrated the presence of intact 4PEG–DX-1000 in circulation one or more days postadministration (data not shown). From the pharmacokinetic data obtained in mice and rabbits, we estimated a circulating half-life for 4PEG–DX-1000 of about 14 days in humans [35,36].

4PEG–DX-1000 Blocks Human Breast Cancer Growth and Tumor Metastasis In Vivo

MDA-MB-231 cells stably transfected with GFP have similar growth and invasive characteristics to wild type cells and allow for the determination of the number and size of microscopic GFP-positive cells [31,37]. 4PEG–DX-1000 administration as monotherapy resulted in a significant decrease of primary tumor growth (~43%) ($P < .05$) with 4PEG–DX-1000 at 10 mg/kg ($P < .05$) without any noticeable side effects including any change in body weight (Figure 4*A*).

To evaluate the effect of 4PEG–DX-1000 on MDA-MB-231 tumor metastasis *in vivo*, at the end of these studies control and experimental animals were sacrificed, lungs, liver, and spleen were removed and the presence of GFP-positive tumor cells was assessed. Animals inoculated with MDA-MB-231–GFP cells and treated with 4PEG–DX-1000 (10 mg/kg) developed significantly less number of microscopic tumor metastases in their lungs and liver compared to control animals receiving vehicle alone (Figure 4*B*).

4PEG–DX-1000 Treatment Leads to a Significant Reduction of Plasminogen and uPA Expression in MDA-MB-231 Tumors

To further assess plasminogen and uPA expression, we examined the MDA-MB-231 tumors growing orthotopically by uPA and plasminogen immunohistochemical analysis to determine whether 4PEG–DX-1000 treatment modulated their expression. We found that 4PEG–DX-1000 treatment reduced uPA and plasminogen expression by 55% and 63%, respectively, compared with the control-treated group (Figure 5).

4PEG–DX-1000 Treatment Leads to a Significant Inhibition of Tumor Cell Proliferation and a Decrease of Tumor Vessel Hot Spots

Sections from 4PEG–DX-1000–treated tumors had ~52% less Ki-67–positive tumor cells than sections from control-treated animals. Based on the ability of 4PEG–DX-1000 to inhibit angiogenesis *in vitro* (Figure 2*D*), we sought to evaluate whether 4PEG–DX-1000 had any effect on tumor vessel formation *in vivo*. Sections from 4PEG–DX-1000–treated animals had ~55% ($P < .05$) less CD31-positive hot spots than sections from control-treated animals (Figure 5).

Table 2. Rabbit Plasma Clearance.

Compound	α Phase Clearance (%)	α Phase Half-Life (minutes)	β Phase Clearance (%)	β Phase Half-Life	
				Minutes	Hours
DX-1000	85	0.9	15	61	1.0
4PEG–DX-1000	48	123.0	52	3520	59.0

4PEG–DX-1000 Inhibitory Effects Are Mediated by the MAPK Signaling Pathways

Expression of MAPK and pMAPK were determined and quantified on histologic sections of MDA-MB-231 tumors from treated animals. We found a ~56% ($P < .05$) decreased level of active p38–MAPK in the 4PEG–DX-1000 sections whereas the total p38–MAPK levels were only ~19% less compared to control (Figure 5).

Discussion

Implication of pln in the major stages of cancer progression [42,43] has fueled interest in the design and evaluation of pln-activated prodrugs [44] and pln inhibitors as novel anticancer therapeutic agents [45]. We used our phage display technology to identify a human Kunitz domain–based inhibitor of pln, DX-1000, which demonstrates high potency and specificity [29]. An inhibitor of pln that specifically blocks tumor growth and metastases, but does not compromise hemostasis, could be of major importance in tumor therapy. DX-1000 had no effect on platelet function as measured by the platelet function and thrombelastograph analyzers and no significant effects on global screening tests of coagulation. Fibrinolysis was inhibited using several different types of test system, but DX-1000 may have weaker effects in plasma or whole blood than in buffer because about two- to four-fold higher concentrations appeared to be necessary to cause inhibition of tPA-stimulated plasma clot lysis compared to that required to inhibit pure pln or euglobulin fractions. In contrast, aprotinin displays lower specificity, causes prolongation of clotting times, influences thrombelastography measurements, and inhibits activated protein C, as well as pln. Side effects caused by nonspecific pln inhibitors could have an impact on cancer therapy. Importantly, DX-1000 demonstrated little effect on coagulation or platelet function in our studies *in vitro*.

Despite significant promise of DX-1000 *in vitro*, chronic administration in human patients would be challenging,

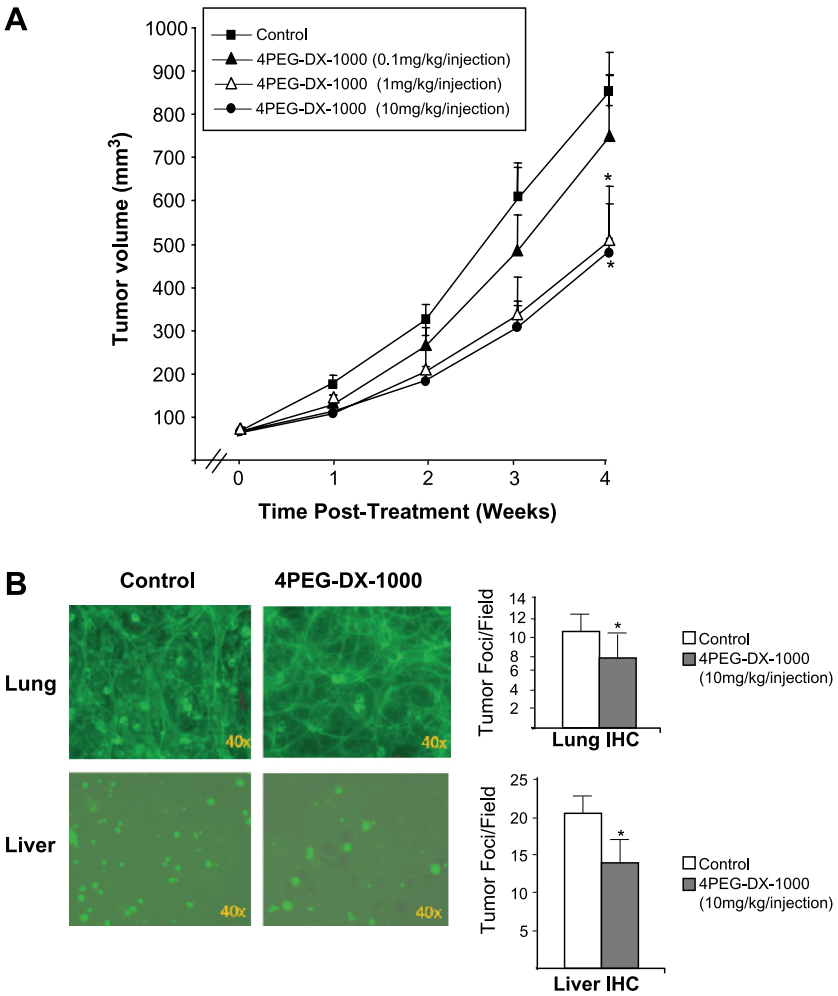

Figure 4. *Effect of 4PEG–DX-1000 on MDA-MB-231–GFP tumor growth and metastasis. MDA-MB-231 tumors were allowed to grow, randomized to average tumor volume of 60 to 70 mm^3 in each group, and treated with 4PEG–DX-1000 (0.1, 1, and 10 mg/kg every day) or with vehicle alone through intraperitoneal route for 4 weeks from the time of randomization of animals. (A) Tumor volume in control and experimental animals was determined at weekly intervals. Significant difference from control was determined by ANOVA and is shown by asterisks (*P < .05). (B) At the end of these studies, lungs and liver from control and experimental animals treated with 4PEG–DX-1000 (10 mg/kg) were removed and the number of metastatic tumor foci was determined as described in the Materials and Methods section. A representative photomicrograph showing metastatic foci is shown. Results are the means ± SEM of 12 animals in each group from two separate experiments. Significant difference in tumor foci was determined by Student's t test and is represented by asterisks (*P < .05).*

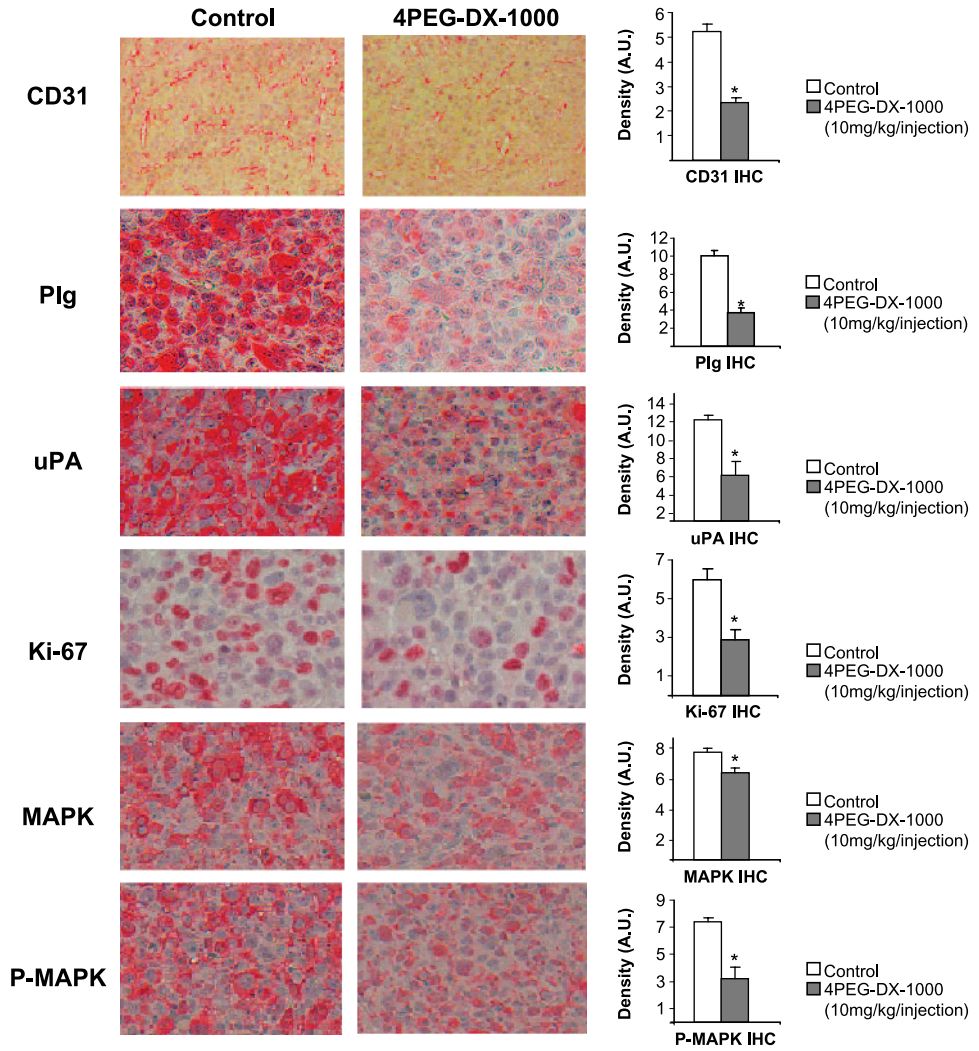

Figure 5. *Effect of 4PEG–DX-1000 on angiogenesis, plg, and uPA expressions, cell proliferation, and MAPK signaling pathway. Immunohistochemical analysis of tumor sections from control and experimental tumors treated with 4PEG–DX-1000 (10 mg/kg) to determine the expression of CD31, uPA, Ki-67, MAPK, and pMAPK. Quantitative analysis was carried out in 10 high-power fields (× 400). Positive staining is seen in red. Change in the levels of expression was quantified by densitometric scanning and expressed as relative density in arbitrary units (A.U.). Results are representative of the mean ± SEM of six animals in each where significant difference from control was determined by ANOVA and shown by asterisks in right-hand panels (*P < .05).*

mostly because of a high clearance and short plasma half-life. To circumvent these problems, PEG moieties have been covalently attached to DX-1000. Our results demonstrated that, by increasing the molecular mass of DX-1000 from ~7 to 27 kDa through the coupling of four 5-kDa PEG moieties, we significantly improved pharmacokinetics of DX-1000 without significantly altering its properties as a pln inhibitor.

When evaluated *in vitro*, both DX-1000 and its PEGylated derivative efficiently blocked proMMP-9 activation in tumor cells. Activation of proMMP-9 by a pln/MMP-3 cascade has been shown previously in a tumor cell model [46]. Our studies demonstrated that DX-1000 and 4PEG–DX-1000 efficiently blocked the activation of proMMP-9 occurring through the pln/MMP-3 cascade. Inhibiting this cascade could be beneficial in cancer therapy as high MMP-9 activity is detected in many tumors including esophageal tumors [47] and pancreatic adenocarcinoma [48]. MMP-9 expression is also associated with a poor prognosis in non–small cell lung cancers [49].

To grow efficiently *in vivo*, tumor cells induce angiogenesis in both primary tumors and metastatic foci [50,51]. Angiogenesis has become a key target in therapeutic strategies aimed at inhibiting tumor growth and other diseases associated with neovascularization [52]. HUVEC and mouse endothelial LEII cells express uPA and are thus able to initiate the proteolytic cascade by converting plg into pln. We demonstrated that DX-1000 and 4PEG–DX-1000 were able to efficiently inhibit tube formation of human and mouse endothelial cells, confirming the critical involvement of pln in the angiogenic process as described by others [24,53–55].

In vivo, we examined MDA-MB-231 cancer cells as an experimental model of an aggressive breast cancer. Accumulating evidence suggests that the components of the plg–pln system are critically involved in invasion and metastasis of breast cancer [42,56–58]. MDA-MB-231 cells are highly invasive and express high levels of uPA and uPAR [59,60]. Blocking uPA/uPAR interaction with a peptide derived from the non–receptor-binding domain of uPA has been shown to

have antiangiogenic and proapoptotic activities *in vivo* [37,61]. Our *in vivo* results demonstrated that, as monotherapy, 4PEG–DX-1000 caused a significant reduction of MDA-MB-231 primary tumor growth. We also examined metastases in distant organs and show that in the lungs and liver of treated animals, the number of MDA-MB-231–GFP cells is significantly reduced compared to that in the control animals. Immunocytochemical analysis of the 4PEG–DX-1000-treated tumor sections showed that this tumor growth inhibition was associated with a significant reduction of CD31-positive hot spots and a significant reduction of plg and uPA expression. High levels of uPA and its inhibitor plasminogen activator type 1 are associated with early relapse and poor overall survival independent of tumor grade, tumor size, and hormone receptor status [62–64]. Stillfried et al. [65] showed that the invasive capacity of breast cancer cells may be linked to the presence of high levels of active uPA, which, in concert with bound plg, can generate large amounts of pln at the cell surface through a positive feedback mechanism. Our results show that blocking pln is sufficient to substantially reduce the levels of plg and uPA in a tumor microenvironment. Immunocytochemical Ki-67 staining of tumor sections also indicated a strong decrease of cellular proliferation activity associated with a decrease in phosphorylation of p38–MAPK in tumor sections from 4PEG–DX-1000–treated animals, demonstrating that tumor growth is modulated through the MAPK pathway as described by others [66].

Whereas further in-depth studies will elucidate the mode of action of 4PEG–DX-1000, antitumor effects reported in the current study can be attributed, in part, to the ability of 4PEG–DX-1000 to block plasmin-mediated activation of several proteases (including MMPs and uPA) and latent growth factors which can regulate the expression of these proteins. It has been described by others that the p38–MAPK signaling pathway is involved in the regulation of uPA/uPAR expression and breast cancer cell invasion [67]. Our hypothesis is that 4PEG–DX-1000 indirectly diminishes uPA expression through the p38–MAPK pathway. Both direct (plasmin inhibition) and indirect (downregulation of the uPA/uPAR system) effects of 4PEG–DX-1000 could explain the antitumoral, antimetastatic, and antiangiogenic effects that we observed.

4PEG–DX-1000 potently inhibits human pln and represents an attractive new antiproteolytic and antiangiogenic drug candidate. Our demonstration that 4PEG–DX-1000 can retard tumor progression and metastasis in a breast cancer model provides a rationale for its evaluation as an antineoplastic agent.

Acknowledgements

We are very grateful to Kari Alitalo (Molecular/Cancer Biology Laboratory, Haartman Institute and Biomedicum Helsinki, University of Helsinki, Finland) who kindly provided the LEII cells.

References

[1] Saksela O (1985). Plasminogen activation and regulation of pericellular proteolysis. *Biochim Biophys Acta* **823**, 35–65.
[2] Vassalli JD and Pepper MS (1994). Tumour biology. Membrane proteases in focus. *Nature* **370**, 14–15.
[3] Parfyonova YV, Plekhanova OS, and Tkachuk VA (2002). Plasminogen activators in vascular remodeling and angiogenesis. *Biochemistry (Mosc)* **67**, 119–134.
[4] Lijnen HR (2001). Elements of the fibrinolytic system. *Ann N Y Acad Sci* **936**, 226–236.
[5] Kolev K, Lerant I, Tenekejiev K, and Machovich R (1994). Regulation of fibrinolytic activity of neutrophil leukocyte elastase, plasmin, and miniplasmin by plasma protease inhibitors. *J Biol Chem* **269**, 17030–17034.
[6] Pollanen J, Stephens RW, and Vaheri A (1991). Directed plasminogen activation at the surface of normal and malignant cells. *Adv Cancer Res* **57**, 273–328.
[7] Dano K, Romer J, Nielsen BS, Bjorn S, Pyke C, Rygaard J, and Lund LR (1999). Cancer invasion and tissue remodeling—cooperation of protease systems and cell types. *APMIS* **107**, 120–127.
[8] Rosmann S, Hahn D, Lottaz D, Kruse MN, Stocker W, and Sterchi EE (2002). Activation of human meprin-alpha in a cell culture model of colorectal cancer is triggered by the plasminogen-activating system. *J Biol Chem* **277**, 40650–40658.
[9] Dano K, Andreasen PA, Grondahl-Hansen J, Kristensen P, Nielsen LS, and Skriver L (1985). Plasminogen activators, tissue degradation, and cancer. *Adv Cancer Res* **44**, 139–266.
[10] Mignatti P, Mazzieri R, and Rifkin DB (1991). Expression of the urokinase receptor in vascular endothelial cells is stimulated by basic fibroblast growth factor. *J Cell Biol* **113**, 1193–1201.
[11] Plow EF, Herren T, Redlitz A, Miles LA, and Hoover-Plow JL (1995). The cell biology of the plasminogen system. *FASEB J* **9**, 939–945.
[12] Plow EF and Miles LA (1990). Plasminogen receptors in the mediation of pericellular proteolysis. *Cell Differ Dev* **32**, 293–298.
[13] Cox G, Steward WP, and O'Byrne KJ (1999). The plasmin cascade and matrix metalloproteinases in non–small cell lung cancer. *Thorax* **54**, 169–179.
[14] Skrzydlewska E, Sulkowska M, Koda M, and Sulkowski S (2005). Proteolytic–antiproteolytic balance and its regulation in carcinogenesis. *World J Gastroenterol* **11**, 1251–1266.
[15] Liotta LA, Goldfarb RH, Brundage R, Siegal GP, Terranova V, and Garbisa S (1981). Effect of plasminogen activator (urokinase), plasmin, and thrombin on glycoprotein and collagenous components of basement membrane. *Cancer Res* **41**, 4629–4636.
[16] Makowski GS and Ramsby ML (1999). Amorphous calcium phosphate–mediated binding of matrix metalloproteinase-9 to fibrin is inhibited by pyrophosphate and bisphosphonate. *Inflammation* **23**, 333–360.
[17] Festuccia C, Dolo V, Guerra F, Violini S, Muzi P, Pavan A, and Bologna M (1998). Plasminogen activator system modulates invasive capacity and proliferation in prostatic tumor cells. *Clin Exp Metastasis* **16**, 513–528.
[18] Simian M, Hirai Y, Navre M, Werb Z, Lochter A, and Bissell MJ (2001). The interplay of matrix metalloproteinases, morphogens and growth factors is necessary for branching of mammary epithelial cells. *Development* **128**, 3117–3131.
[19] Mazzieri R, Masiero L, Zanetta L, Monea S, Onisto M, Garbisa S, and Mignatti P (1997). Control of type IV collagenase activity by components of the urokinase–plasmin system: a regulatory mechanism with cell-bound reactants. *EMBO J* **16**, 2319–2332.
[20] Montrucchio G, Lupia E, De Martino A, Silvestro L, Savu SR, Cacace G, De Filippi PG, Emanuelli G, and Camussi G (1996). Plasmin promotes an endothelium-dependent adhesion of neutrophils. Involvement of platelet activating factor and P-selectin. *Circulation* **93**, 2152–2160.
[21] Folkman J (1993). Diagnostic and therapeutic applications of angiogenesis research. *C R Acad Sci III* **316**, 909–918.
[22] Weidner N, Folkman J, Pozza F, Bevilacqua P, Allred EN, Moore DH, Meli S, and Gasparini G (1992). Tumor angiogenesis: a new significant and independent prognostic indicator in early-stage breast carcinoma. *J Natl Cancer Inst* **84**, 1875–1887.
[23] Lee S, Jilani SM, Nikolova GV, Carpizo D, and Iruela-Arispe ML (2005). Processing of VEGF-A by matrix metalloproteinases regulates bioavailability and vascular patterning in tumors. *J Cell Biol* **169**, 681–691.
[24] McColl BK, Baldwin ME, Roufail S, Freeman C, Moritz RL, Simpson RJ, Alitalo K, Stacker SA, and Achen MG (2003). Plasmin activates the lymphangiogenic growth factors VEGF-C and VEGF-D. *J Exp Med* **198**, 863–868.

[25] Falcone DJ, McCaffrey TA, Haimovitz-Friedman A, Vergilio JA, and Nicholson AC (1993). Macrophage and foam cell release of matrix-bound growth factors. Role of plasminogen activation. *J Biol Chem* **268**, 11951–11958.

[26] Saksela O and Rifkin DB (1990). Release of basic fibroblast growth factor–heparan sulfate complexes from endothelial cells by plasminogen activator–mediated proteolytic activity. *J Cell Biol* **110**, 767–775.

[27] Mars WM, Zarnegar R, and Michalopoulos GK (1993). Activation of hepatocyte growth factor by the plasminogen activators uPA and tPA. *Am J Pathol* **143**, 949–958.

[28] Cines DB, Pollak ES, Buck CA, Loscalzo J, Zimmerman GA, McEver RP, Pober JS, Wick TM, Konkle BA, Schwartz BS, et al. (1998). Endothelial cells in physiology and in the pathophysiology of vascular disorders. *Blood* **91**, 3527–3561.

[29] Markland W, Ley AC, Lee SW, and Ladner RC (1996). Iterative optimization of high-affinity proteases inhibitors using phage display: 1. Plasmin. *Biochemistry* **35**, 8045–8057.

[30] Robbie LA, Booth NA, Croll AM, and Bennett B (1993). The roles of alpha 2-antiplasmin and plasminogen activator inhibitor 1 (PAI-1) in the inhibition of clot lysis. *Thromb Haemost* **70**, 301–306.

[31] Pakneshan P, Szyf M, Farias-Eisner R, and Rabbani SA (2004). Reversal of the hypomethylation status of urokinase (uPA) promoter blocks breast cancer growth and metastasis. *J Biol Chem* **279**, 31735–31744.

[32] Maquoi E, Frankenne F, Noel A, Krell HW, Grams F, and Foidart JM (2000). Type IV collagen induces matrix metalloproteinase 2 activation in HT1080 fibrosarcoma cells. *Exp Cell Res* **261**, 348–359.

[33] Chizzonite R, Truitt T, Desai BB, Nunes P, Podlaski FJ, Stern AS, and Gately MK (1992). IL-12 receptor: I. Characterization of the receptor on phytohemagglutinin-activated human lymphoblasts. *J Immunol* **148**, 3117–3124.

[34] Chizzonite R, Truitt T, Podlaski FJ, Wolitzky AG, Quinn PM, Nunes P, Stern AS, and Gately MK (1991). IL-12: monoclonal antibodies specific for the 40-kDa subunit block receptor binding and biologic activity on activated human lymphoblasts. *J Immunol* **147**, 1548–1556.

[35] Mahmood I and Balian JD (1999). The pharmacokinetic principles behind scaling from preclinical results to phase I protocols. *Clin Pharmacokinet* **36**, 1–11.

[36] Mahmood I and Balian JD (1996). Interspecies scaling: a comparative study for the prediction of clearance and volume using two or more than two species. *Life Sci* **59**, 579–585.

[37] Guo Y, Higazi AA, Arakelian A, Sachais BS, Cines D, Goldfarb RH, Jones TR, Kwaan H, Mazar AP, and Rabbani SA (2000). A peptide derived from the nonreceptor binding region of urokinase plasminogen activator (uPA) inhibits tumor progression and angiogenesis and induces tumor cell death *in vivo*. *FASEB J* **14**, 1400–1410.

[38] Shukeir N, Arakelian A, Kadhim S, Garde S, and Rabbani SA (2003). Prostate secretory protein PSP-94 decreases tumor growth and hypercalcemia of malignancy in a syngenic *in vivo* model of prostate cancer. *Cancer Res* **63**, 2072–2078.

[39] Pizzi H, Gladu J, Carpio L, Miao D, Goltzman D, and Rabbani SA (2003). Androgen regulation of parathyroid hormone–related peptide production in human prostate cancer cells. *Endocrinology* **144**, 858–867.

[40] Chen G, Shukeir N, Potti A, Sircar K, Aprikian A, Goltzman D, and Rabbani SA (2004). Up-regulation of Wnt-1 and beta-catenin production in patients with advanced metastatic prostate carcinoma: potential pathogenetic and prognostic implications. *Cancer* **101**, 1345–1356.

[41] Ley AC, Markland W, and Ladner RC (1996). Obtaining a family of high-affinity, high-specificity protein inhibitors of plasmin and plasma kallikrein. *Mol Divers* **2**, 119–124.

[42] Foekens JA, Peters HA, Look MP, Portengen H, Schmitt M, Kramer MD, Brunner N, Janicke F, Meijer-van Gelder ME, Henzen-Logmans SC, et al. (2000). The urokinase system of plasminogen activation and prognosis in 2780 breast cancer patients. *Cancer Res* **60**, 636–643.

[43] Noel A, Albert V, Bajou K, Bisson C, Devy L, Frankenne F, Maquoi E, Masson V, Sounni NE, and Foidart JM (2001). New functions of stromal proteases and their inhibitors in tumor progression. *Surg Oncol Clin N Am* **10**, 417–432, x–xi.

[44] Devy L, de Groot FM, Blacher S, Hajitou A, Beusker PH, Scheeren HW, Foidart JM, and Noel A (2004). Plasmin-activated doxorubicin prodrugs containing a spacer reduce tumor growth and angiogenesis without systemic toxicity. *FASEB J* **18**, 565–567.

[45] Jedinak A and Maliar T (2005). Inhibitors of proteases as anticancer drugs. *Neoplasma* **52**, 185–192.

[46] Hahn-Dantona E, Ramos-DeSimone N, Sipley J, Nagase H, French DL, and Quigley JP (1999). Activation of proMMP-9 by a plasmin/MMP-3 cascade in a tumor cell model. Regulation by tissue inhibitors of metalloproteinases. *Ann N Y Acad Sci* **878**, 372–387.

[47] Kumagai Y, Toi M, and Inoue H (2002). Dynamism of tumour vasculature in the early phase of cancer progression: outcomes from oesophageal cancer research. *Lancet Oncol* **3**, 604–610.

[48] Duxbury MS, Ito H, Benoit E, Ashley SW, and Whang EE (2004). CEACAM6 is a determinant of pancreatic adenocarcinoma cellular invasiveness. *Br J Cancer* **91**, 1384–1390.

[49] Swinson DE, Cox G, and O'Byrne KJ (2004). Coexpression of epidermal growth factor receptor with related factors is associated with a poor prognosis in non–small-cell lung cancer. *Br J Cancer* **91**, 1301–1307.

[50] Folkman J (2002). Role of angiogenesis in tumor growth and metastasis. *Semin Oncol* **29**, 15–18.

[51] Folkman J (1985). Tumor angiogenesis. *Adv Cancer Res* **43**, 175–203.

[52] Rakic JM, Maillard C, Jost M, Bajou K, Masson V, Devy L, Lambert V, Foidart JM, and Noel A (2003). Role of plasminogen activator–plasmin system in tumor angiogenesis. *Cell Mol Life Sci* **60**, 463–473.

[53] Baker EA, Bergin FG, and Leaper DJ (2000). Plasminogen activator system, vascular endothelial growth factor, and colorectal cancer progression. *Mol Pathol* **53**, 307–312.

[54] Cherrington JM, Strawn LM, and Shawver LK (2000). New paradigms for the treatment of cancer: the role of anti–angiogenesis agents. *Adv Cancer Res* **79**, 1–38.

[55] Wang H, Schultz R, Hong J, Cundiff DL, Jiang K, and Soff GA (2004). Cell surface–dependent generation of angiostatin4.5. *Cancer Res* **64**, 162–168.

[56] Grondahl-Hansen J, Christensen IJ, Rosenquist C, Brunner N, Mouridsen HT, Dano K, and Blichert-Toft M (1993). High levels of urokinase-type plasminogen activator and its inhibitor PAI-1 in cytosolic extracts of breast carcinomas are associated with poor prognosis. *Cancer Res* **53**, 2513–2521.

[57] Stephens RW, Brunner N, Janicke F, and Schmitt M (1998). The urokinase plasminogen activator system as a target for prognostic studies in breast cancer. *Breast Cancer Res Treat* **52**, 99–111.

[58] Garbett EA, Reed MW, Stephenson TJ, and Brown NJ (2000). Proteolysis in human breast cancer. *Mol Pathol* **53**, 99–106.

[59] Seddighzadeh M, Zhou JN, Kronenwett U, Shoshan MC, Auer G, Sten-Linder M, Wiman B, and Linder S (1999). ERK signalling in metastatic human MDA-MB-231 breast carcinoma cells is adapted to obtain high urokinase expression and rapid cell proliferation. *Clin Exp Metastasis* **17**, 649–654.

[60] Holst-Hansen C, Johannessen B, Hoyer-Hansen G, Romer J, Ellis V, and Brunner N (1996). Urokinase-type plasminogen activation in three human breast cancer cell lines correlates with their *in vitro* invasiveness. *Clin Exp Metastasis* **14**, 297–307.

[61] Guo Y, Mazar AP, Lebrun JJ, and Rabbani SA (2002). An antiangiogenic urokinase-derived peptide combined with tamoxifen decreases tumor growth and metastasis in a syngeneic model of breast cancer. *Cancer Res* **62**, 4678–4684.

[62] Corte MD, Verez P, Rodriguez JC, Roibas A, Dominguez ML, Lamelas ML, Vazquez J, Garcia Muniz JL, Allende MT, Gonzalez LO, et al. (2005). Tissue-type plasminogen activator (tPA) in breast cancer: relationship with clinicopathological parameters and prognostic significance. *Breast Cancer Res Treat* **90**, 33–40.

[63] Duffy MJ (2004). The urokinase plasminogen activator system: role in malignancy. *Curr Pharm Des* **10**, 39–49.

[64] Harbeck N, Kates RE, Gauger K, Willems A, Kiechle M, Magdolen V, and Schmitt M (2004). Urokinase-type plasminogen activator (uPA) and its inhibitor PAI-I: novel tumor-derived factors with a high prognostic and predictive impact in breast cancer. *Thromb Haemost* **91**, 450–456.

[65] Stillfried GE, Saunders DN, and Ranson M (2007). Plasminogen binding and activation at the breast cancer cell surface: the integral role of urokinase activity. *Breast Cancer Res* **9**, R14.

[66] Gandhari M, Arens N, Majety M, Dorn-Beineke A, and Hildenbrand R (2006). Urokinase-type plasminogen activator induces proliferation in breast cancer cells. *Int J Oncol* **28**, 1463–1470.

[67] Chen J, Baskerville C, Han Q, Pan ZK, and Huang S (2001). Alpha(v) integrin, p38 mitogen-activated protein kinase, and urokinase plasminogen activator are functionally linked in invasive breast cancer cells. *J Biol Chem* **276**, 47901–47905.